

Flavor tagging TeV jets for BSM and QCD

KEITH PEDERSEN¹ AND ZACK SULLIVAN*Department of Physics
Illinois Institute of Technology
Chicago, Illinois 60616-3793, USA***Abstract**

We present a new scheme for tagging high- p_T bottom and charm jets using energetic muons. Contemporary track-based b tags lose their ability to reject light jet background as jet $p_T \rightarrow \mathcal{O}(\text{TeV})$, where the massive boost exposes fundamental limits in tracking resolution. For our “ μ_x ” tag, the signal efficiency *and* light jet rejection is robust versus p_T . In the tested regime (jet $p_T \in [0.5, 2.1]$ TeV), μ_x tags $\sim 14\%$ of b jets, $\sim 6.5\%$ of c jets and $\sim 0.65\%$ of light jets. Since μ_x tagging should be immediately useful in a searches for heavy resonances, we test it with a typical dijet search — a heavy, leptophobic Z' .

PRESENTED AT

DPF 2015

The Meeting of the American Physical Society
Division of Particles and Fields
Ann Arbor, Michigan, August 4–8, 2015

¹Presenting author. kpeders1@hawk.iit.edu

1 Introduction

Searches for physics beyond the standard model (BSM) are a major focus of research at the LHC. A common signature of BSM physics is a dijet resonance, which naturally sits atop an enormous QCD background. Perhaps the most direct way to enhance the purity of such a signal is to flavor tag the dijets. For instance, isolating the $b\bar{b}$ channel will slash the dominant light jet background — provided that the b tag can reject light jets.

Heavy jets (c or b initiated) and light jets (d , u , s or g initiated) are distinguishable from their underlying partonic physics. The large mass of heavy quarks ($m \gtrsim \Lambda_{QCD}$) discourages fragmentation, so their hadrons often carry the majority of the jet’s momentum. Their proper life-distance is $\mathcal{O}(0.5\text{ mm})$, which displaces their decay vertices a *measurable* distance from primary vertex of the hard scatter, but at least 50 times closer than more common light hadrons (e.g. $c\tau(K_S^0) \approx 27\text{ mm}$). And their large rate of semi-leptonic decay ($\mathcal{B}(Y_{b/c} \rightarrow l^+\nu_l X) \approx 0.1$ for each $l \in \{e, \mu\}$) enriches their jets with energetic leptons.

These properties are leveraged at the LHC in the two main classes of flavor tagging.

- *Track tagging* looks for charged tracks inside a jet that converge at a secondary vertex (SV) noticeably displaced from the primary vertex. Using the SV’s properties (displacement distance, reconstructed mass, etc.), jets likely to contain a heavy hadron are tagged.
- *p_T^{rel} tagging* measures a lepton’s momentum transverse to the centroid of its jet. Heavy jets contain more leptons, and these should have larger values of p_T^{rel} because: (i) the large mass of its mother causes the lepton to be emitted at wider angles and (ii) heavy hadrons carry a larger fraction of the jet’s momentum, producing more energetic leptons. However, p_T^{rel} generally only works for *muons*, as background electrons are too numerous inside a jet, which is already an environment where electron identification is difficult.

Charm jets perform much weaker in both tags because: (i) c hadrons have shorter lifetimes and smaller masses and (ii) b hadrons primarily decay to c hadrons, giving b jets twice as many muons and a second chance to create displaced tracks. Thus, both tags are generally considered b tags with a higher fake rate for c jets than light jets.

As jet $p_T \rightarrow \mathcal{O}(\text{TeV})$, both tags lose much of their ability to reject light jet background. Here, the extreme boost collimates the jet so much that SV properties become very sensitive to tracking resolution [1, 2]. Similarly, p_T^{rel} distributions for muons in heavy and light jets become nearly indistinguishable [3]. However, while the loss of purity for the track tag is primarily a detector effect, the failure of p_T^{rel} is predictable from the underlying kinematics of boosted semi-muonic decay.

2 A new heavy flavor tag

Consider a jet containing a B hadron. In the center-of-momentum (CM) frame, a muon is emitted with some speed $\beta_{\mu,\text{cm}}$ and at some angle θ_{cm} w.r.t. the boost axis (see Fig. 1). In the lab frame, the boost γ_B compresses the decay products into a subjet. Using $\kappa \equiv \beta_B/\beta_{\mu,\text{cm}}$, we can define a lab frame observable

$$x \equiv \gamma_B \tan(\theta_{\text{lab}}) = \frac{\sin(\theta_{\text{cm}})}{\kappa + \cos(\theta_{\text{cm}})} \quad . \quad (1)$$

When the muon and the b hadron are both relativistic, $\kappa \approx 1$ and x is nearly invariant. Since we are only interested in b jets where $\gamma_B \gg \gamma_{\mu,\text{cm}}$, we only consider the *over-*boosted ($\kappa \geq 1$) distribution for count N (where $x \in [0, 1/\sqrt{\kappa^2 - 1}]$),

$$\frac{dN}{dx} = 4\pi \frac{2x}{(x^2 + 1)^2} K(x, \kappa) \quad \text{with} \quad (2)$$

$$K(x, \kappa) = \frac{(1 + \kappa^2) + x^2(1 - \kappa^2)}{2\sqrt{1 + x^2(1 - \kappa^2)}} \quad . \quad (3)$$

Here, $K(x, \kappa)$ corrects the nominal shape when $\kappa > 1$.

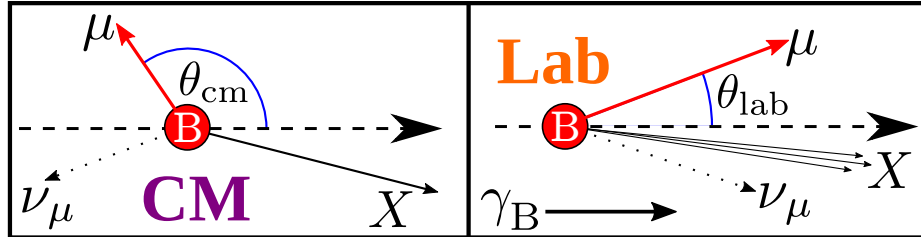


Figure 1: Boosted nomenclature.

Figure 2a demonstrates that the $K(x, \kappa)$ correction is small for most $\gamma_{\mu,\text{cm}}$. This is further exemplified in Fig. 2b, where an ensemble of decays “integrates” over the $\gamma_{\mu,\text{cm}}$ spectrum, while essentially preserving the nominal shape ($\kappa = 1$, dotted line) of Eq. (2). The downward correction in the tail, from each muon’s boost cone boundary, is fit by adding a Logistic curve to the nominal shape (to act as a cut-off function), along with a normalization factor C .

These results support the calculation that, if most muons are relativistic in the CM frame, at least 90% will arrive in a cone defined by $x \leq 3$. This cone can be used to accept/exclude muons which are consistent with boosted semi-muonic decay, forming the basis for a new b tag. Most notably, the *physical* size of this cone should decrease as jet p_T increases, underlying the failure of p_T^{rel} ; muons from *very* boosted b hadrons should no longer arrive at wide angles.

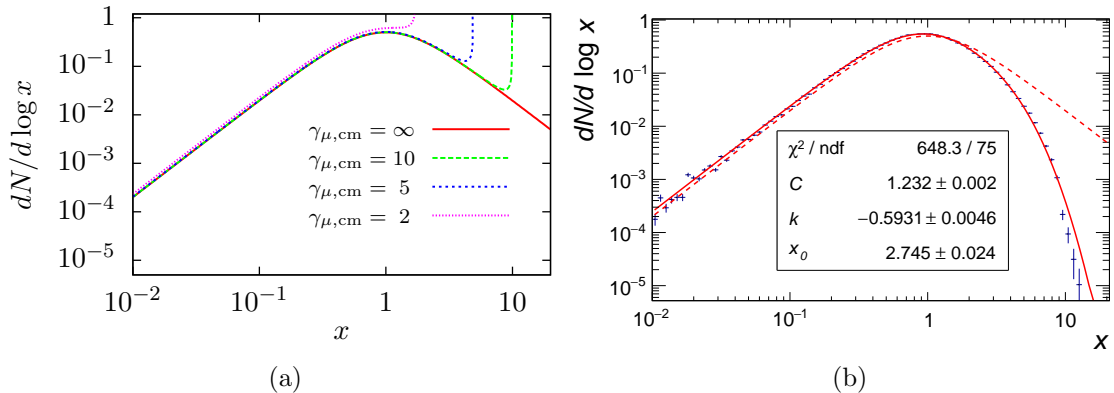


Figure 2: (a) Theoretical $dN/d \log x$ for muons of various $\gamma_{\mu, \text{cm}}$ and (b) $dN/d \log x$ for muons inside simulated b jets.

2.1 Measuring x

Measuring x requires reconstructing the four-momentum of the semi-muonic decay,

$$\mathbf{p}_{\text{subject}} = \mathbf{p}_{\text{core}} + \mathbf{p}_{\mu} + \mathbf{p}_{\nu_{\mu}} \approx \mathbf{p}_{\text{core}} + 2\mathbf{p}_{\mu} \quad , \quad (4)$$

where the “core” is composed of the boosted hadronic remnants (the X in Fig. 1). Since most of the ν_{μ} ’s lab frame momentum is from its mother’s boost, the muon is an acceptable proxy (with the simplest choice being $\mathbf{p}_{\nu_{\mu}} = \mathbf{p}_{\mu}$).

Tracks provide the best angular information to reconstruct the thin core, but its high collimation will hamper track finding in a non-trivial way. To simplify detector simulation, we build jets (and cores) solely from calorimeter towers and muons. To mitigate the coarse granularity of the hadronic calorimeter (HCal), we use the finer granularity of the the EM Calorimeter (ECal) to orient the combined towers (“ECal pointing”). This assumes that cores likely contain boosted photons/electrons (especially from π^0), and most hadrons begin showering in the ECal.

Jets containing muons are reclustered with anti- k_T to produces a list of candidate cores. The fixed tower width w requires using $\sqrt{2}w < R_{\text{core}} < 2w$ to capture the core in a 3×3 grid (the smallest choice which can triangulate an impact). Since this granularity produces an ill-measured mass, we fix each candidate to m_{core} (the expected mass under the b hadron hypothesis). The “correct” core is the one which, when the muon is added twice, produces a subjet whose mass is closest to m_B , the nominal mass of the b hadron admixture. As a final sanity test, the momentum fraction of the subjet

$$f_{\text{subject}} = \frac{p_{T, \text{subject}}}{p_{T, \text{jet}}} \quad , \quad (5)$$

should be close to one, since b quarks shun hard radiation.

2.2 The μ_x tag

The μ_x tag uses four basic cuts: (i) $p_{T,\mu} \geq 10$ GeV ensures that the muon is well reconstructed, (ii) jet $p_T \geq 300$ GeV confirms that boosted kinematics apply, (iii) $x \leq 3$ establishes that the muon is consistent with a boosted primordial decay, given its local jet environment and (iv) $f_{\text{subjet}} \geq 0.5$ verifies that the subjet is consistent with a heavy quark.

We test the μ_x tag by generating samples of $b\bar{b}$, $c\bar{c}$, and $j\bar{j}$ (where $j \in \{u, d, s, g\}$), spanning $p_T = 0.1$ – 2.1 TeV, with MADGRAPH5 [4]. We fragment and hadronize in PYTHIA 8 [5,6] and model the ATLAS detector with DELPHES 3 [7], clustering jets with FastJet 3 [8]. Pileup is generated by PYTHIA, using the parameters suggested by ATLAS in Ref. [9], and a random number of pileup events (drawn from a Poisson distribution with $\mu = 40$) are added to each event.

Muons are simulated as “standalone” tracks, which only use hits from the ATLAS Muon Spectrometer (MS). In order to implement “ECal pointing” in the DELPHES Calorimeter module, we use the granularity of ATLAS ECal Layer 2 (0.025×0.025) for the region overlapping the MS ($|\eta| < 2.7$). Jets are clustered from towers and muons using anti- k_T with $R = 0.4$. The subjets of those containing muons are built using $R_{\text{core}} = 0.04$, $m_{\text{core}} = 2$ GeV, and $m_B = 5.3$ GeV. To prevent x from growing absurdly small, we use $\gamma_B = E_{\text{subjet}} / \min(m_{\text{subjet}}, 12 \text{ GeV})$.

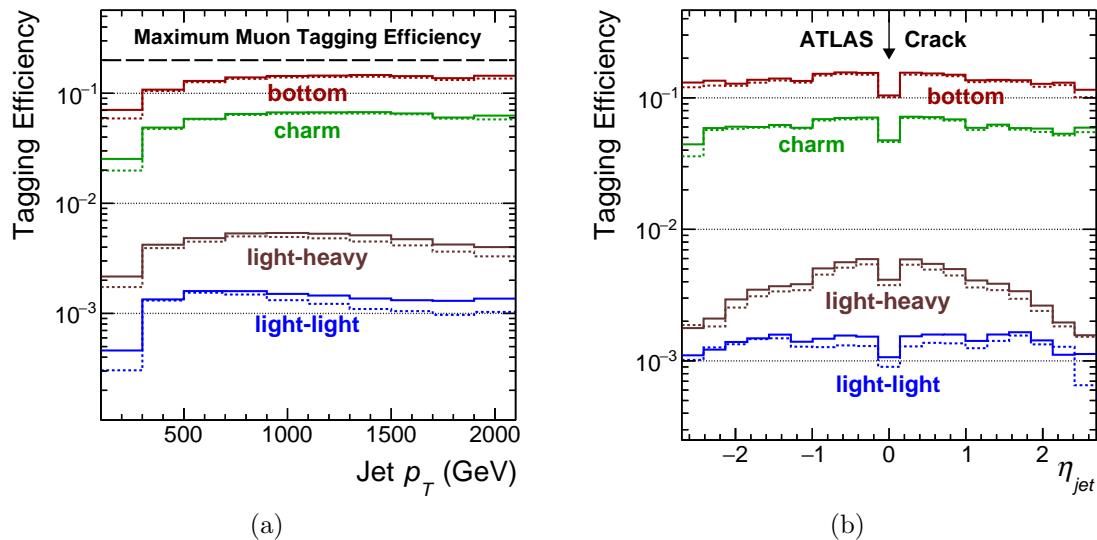


Figure 3: μ_x tagging efficiency without pileup (solid) and with $\mu = 40$ (dashed) versus (a) jet p_T and (b) η_{jet} .

In Fig. 3 we show the efficiency to tag the top two jets (ranked by p_T) in each event. Light jets are split into two classes, where *light-heavy* is a jet initiated by

a light parton, but whose muon originated from a heavy hadron (i.e. a gluon split to heavy quarks during fragmentation). Once the boosted approximations turn on ($\kappa \approx 1$), the efficiency to tag heavy jets is both flat versus p_T and insensitive to pileup. Fig. 3b only uses jets with $p_T \geq 300$ GeV, leading to poor statistics at the edge of the MS; nonetheless, the efficiency to tag heavy jets is also relatively flat with η_{jet} (excluding ATLAS’s central detector services crack, where standalone muon efficiency plummets).

3 Leptophobic Z'

One of the simplest BSM models is an additional $U(1)'$ symmetry mediated by a heavy, neutral Z' . Since the LHC has already probed large scales in the “golden” channel (dileptons) and seen no such resonance, the simplest $U(1)'$ are excluded. But if the new symmetry is associated with baryon number, only SM quarks would be charged. Anomaly cancellation requires this $U(1)'_B$ to come with new, vector-like quarks and at least one scalar field whose VEV breaks the symmetry [10, 11]. If the vector-like quarks are kinematically inaccessible at the LHC, then the $Z'_{B\mu}$ gauge coupling to SM quarks [10]

$$\frac{g_B}{6} Z'_{B\mu} \bar{q} \gamma^\mu q \quad , \quad (6)$$

would be the only experimental signature of the $U(1)'_B$ at leading order. Since μ_x tagging can greatly enhance the purity of such a dijet signal, we simulate a “bump hunt” at ATLAS Run II (i.e. looking for an excess in $d\sigma/dm_{jj}$). We use two classes: 1-tag and 2-tag (where N -tag requires tagging at least N of the top two jets, ranked by p_T).

The relevant signal is $pp \rightarrow Z'_B \rightarrow b\bar{b}/c\bar{c}(+j)$, where the optional light jet radiation enhances the signal cross section. The relevant background for each class is purely QCD; yet while both classes use $pp \rightarrow b\bar{b}/c\bar{c}/jj(+j)$, the 1-tag class also draws heavily from the bottom/charm PDF via $jh \rightarrow jh(+j)$ (a heavy quark scattering from a light parton). We generate all samples at $\sqrt{s} = 13$ TeV using CT14llo PDFs [12], improving their differential cross sections by using MLM matching between MadGraph and Pythia (in “shower-kt” mode with $q_{cut} \approx M_{Z'_B}/20$) [13]. Signal sets are generated for a range of $M_{Z'_B}$, with corresponding background sets governed by identical kinematic/matching cuts.

Because the μ_x light jet efficiency is minuscule, we approximate the second tag for the light dijet background. This is accomplished by fitting the light jet efficiency as a function of jet p_T and η . When exactly one leading jet is tagged, we find the probability to tag the other jet, then re-weight the event by a factor of $A_1 = \frac{1-\rho/2}{1-\rho}$ or $A_2 = \frac{\rho}{2(1-\rho)}$, for the 1-tag and 2-tag classes, respectively. Light dijet events with two real tags are discarded, to prevent double-counting.

We require $\Delta R_{jj} \leq 1.5$, to suppress t -channel background, and insist that both jets fall within the MS ($|\eta_{jet}| \leq 2.7$). Even though we generate an optional radiation jet, we find that adding a hard third jet to the tagged dijet system causes an unacceptable hardening of the steeply falling QCD continuum. The subsequent loss of the radiation jet, combined with the neutrino estimation inherent to μ_x tagging, smears the dijet mass, requiring a rather wide mass window ($[0.85, 1.25] \times M_{Z'}$) designed to capture nearly all signal above $M_{Z'}$ and as much signal below, while only doubling the background.

We compare the experimental reach of the μ_x tag to existing dijet searches via an exclusion plot [10] for a leptophobic Z'_B (Fig. 4), which demonstrates that — given an expected Run II luminosity of 100 fb^{-1} — the μ_x tag should be sensitive to entirely new regions of model-space.

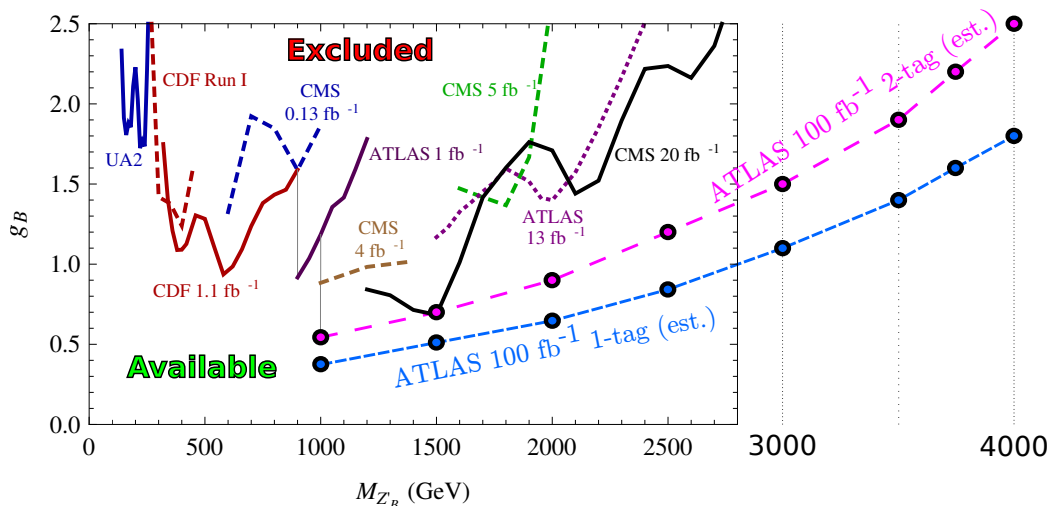


Figure 4: 95% confidence level exclusion limits for Z'_B models.

4 Conclusion

The μ_x tag is a high p_T , heavy flavor tag whose signal efficiency *and* light jet rejection are robust versus p_T . It performs well at identifying a generic heavy quark signal, which suggests it will be useful in a range of applications in BSM physics (especially models which couple predominantly to heavy flavors). Additionally, since μ_x and track tagging are not mutually exclusive, they should be able to cross-check one another in the high p_T regime (a region where track tags are dominated by uncertainties in their tagging efficiency). This should create a combined flavor tag with an overall higher efficiency, a tunable light jet rejection, and much lower uncertainties in its high- p_T tagging efficiency.

ACKNOWLEDGMENTS

This work was supported by the U.S. Department of Energy under Award No. DE-SC0008347.

References

- [1] G. Aad *et al.* [ATLAS Collaboration], ATLAS-CONF-2011-102.
- [2] S. Chatrchyan *et al.* [CMS Collaboration], CMS-PAS-BTV-13-001.
- [3] G. Aad *et al.* [ATLAS Collaboration], ATLAS-CONF-2011-089.
- [4] J. Alwall *et al.*, JHEP **1407**, 079 (2014) [arXiv:1405.0301 [hep-ph]].
- [5] T. Sjostrand, S. Mrenna, and P. Z. Skands, JHEP **0605**, 026 (2006) [hep-ph/0603175].
- [6] T. Sjostrand, S. Mrenna, and P. Z. Skands, Comput. Phys. Commun. **178**, 852 (2008) [arXiv:0710.3820 [hep-ph]].
- [7] J. de Favereau *et al.* [DELPHES 3 Collaboration], JHEP **1402**, 057 (2014) [arXiv:1307.6346 [hep-ex]].
- [8] M. Cacciari, G. P. Salam, and G. Soyez, Eur. Phys. J. C **72**, 1896 (2012) [arXiv:1111.6097 [hep-ph]].
- [9] G. Aad *et al.* [ATLAS Collaboration], ATL-PHYS-PUB-2011-009, ATL-COM-PHYS-2011-744.
- [10] B. A. Dobrescu and F. Yu, Phys. Rev. D **88**, 035021 (2013); Erratum: Phys. Rev. D **90**, 079901 (2014) [arXiv:1306.2629 [hep-ph]].
- [11] B. A. Dobrescu, arXiv:1506.04435 [hep-ph].
- [12] S. Dulat *et al.*, arXiv:1506.07443 [hep-ph].
- [13] J. Alwall, S. de Visscher, and F. Maltoni, JHEP **0902**, 017 (2009) [arXiv:0810.5350 [hep-ph]].